See related commentary on pg 2564

A Targetable, Noncanonical Signal Transducer and Activator of Transcription 3 Activation Induced by the Y-Less Region of IL-22 Receptor Orchestrates Imiquimod-Induced Psoriasis-Like Dermatitis in Mice

Camille Michiels[1], Léna Puigdevall[1], Perrine Cochez[1], Younes Achouri[2], Paméla Cheou[1], Emilie Hendrickx[1], Nicolas Dauguet[3], Christophe Blanchetot[4] and Laure Dumoutier[1]

Exacerbated IL-22 activity induces tissue inflammation and immune disorders such as psoriasis. However, because IL-22 is also essential for tissue repair and defense at barrier interfaces, targeting IL-22 activity to treat psoriasis bears the risk of deleterious effects at mucosal sites such as the gut. We previously showed in vitro that IL-22 signaling relies on IL-22 receptor alpha (IL-22Rα) Y-dependent and -independent pathways. The second depends on the C-terminal Y-less region of IL-22Rα and leads to a massive signal transducer and activator of transcription 3 (STAT3) activation. Because STAT3 activation is associated with the development of psoriasis, we hypothesized that the specific inhibition of the noncanonical STAT3 activation by the Y-less region of IL-22Rα could reduce psoriasis-like disease while leaving intact its tissue defense functions in the gut. We show that mice expressing a C-terminally truncated version of IL-22Rα ($\Delta Cter^{mut/mut}$ mice) are protected from the development of psoriasis-like dermatitis lesions induced by imiquimod to a lesser extent than *Il22ra*$^{-/-}$ mice. In contrast, only *Il22ra*$^{-/-}$ mice lose weight after *Citrobacter rodentium* infection. Altogether, our data suggest that specific targeting of the noncanonical STAT3 activation by IL-22 could serve to treat psoriasis-like skin inflammation without affecting IL-22–dependent tissue repair or barrier defense at other sites.

Journal of Investigative Dermatology (2021) **141,** 2668–2678; doi:10.1016/j.jid.2021.04.016

INTRODUCTION

IL-22 is a member of the IL-10–related cytokine family (Dumoutier et al., 2000a). Depending on the immune context, it can play different roles during inflammatory processes. It exerts essential functions in barrier defense, tissue repair, and homeostasis in various organs, including the skin, gut, lung, and liver (Wolk et al., 2004). However, continuous and/or exacerbated action of IL-22 induces tissue inflammation, leading to immune disorders such as psoriasis. In the inflammatory context, IL-22 is largely produced by T cells, including T helper (Th) 17, Th22, and γδ T cells, as well as by innate lymphoid cells type III (Sabat et al., 2014). IL-22 signals through a receptor composed of two chains: IL-22 receptor alpha (IL-22Rα) and IL-10 receptor β (Kotenko et al., 2001; Xie et al., 2000). Whereas IL-10 receptor β is ubiquitously expressed, IL-22Rα is mainly expressed by epithelial cells, delimiting the cells that respond to IL-22. Once bound to its receptor, IL-22 induces the Jak–signal transducer and activator of transcription (STAT) pathway and, to a lesser extent, the MAPK and protein kinase B pathway (Lejeune et al., 2002).

Jak1 and tyrosine kinase 2, associated respectively with IL-22Rα and IL-10 receptor β, are activated on IL-22 binding (Lejeune et al., 2002). In the classical Jak–STAT pathway, the binding of the cytokine to its receptor induces the trans-activation of the Jaks, preassociated with the receptor. Jak proteins then phosphorylate Y residues of the receptor, which are recognized as docking sites by the Src homology 2 domain of STAT. In turn, these STATs are phosphorylated, inducing their dimerization and migration into the nucleus where they modulate gene expression. The classical Jak–STAT pathway requires the Src homology 2 domain of STAT as well as the Ys of the receptor (Morris et al., 2018); however, in some cases, STAT activation occurs in a phosphotyrosine-independent manner (Dumoutier et al., 2004; Floss et al., 2013; Nicholson et al., 1996; Tian et al., 1996; Ward et al., 1999). For IL-22Rα, we have shown in vitro that the phosphorylation of STAT3 but not of STAT1 or STAT5 could be induced even when all receptor Ys are mutated to phenylalanines (i.e., F). This alternative mode of activation requires the C-terminal (C-ter) part (amino acids 492–574) of IL-22Rα as the truncation of the Y->F mutant abolishes STAT3 activation. Our previous results showed that

[1]*Experimental Medicine Unit, de Duve Institute, Université catholique de Louvain, Brussels, Belgium;* [2]*Transgenic Core Facility, de Duve Institute, Université catholique de Louvain, Brussels, Belgium;* [3]*Flow Cytometry and Cell Sorting Platform, de Duve Institute, Université catholique de Louvain, Brussels, Belgium; and* [4]*Argenx, Ghent, Belgium*

Correspondence: Laure Dumoutier, MEXP, Cytokine Group, de Duve Institute, Université catholique de Louvain, 74 Avenue Hippocrate, Brussels B 1200, Belgium. E-mail: laure.dumoutier@uclouvain.be

Abbreviations: C-ter, C-terminal; crRNA, CRISPR RNA; IL-22Rα, IL-22 receptor alpha; pSTAT, phosphorylated signal transducer and activator of transcription; STAT, signal transducer and activator of transcription; Th, T helper; WT, wild type

Received 18 January 2021; revised 8 April 2021; accepted 22 April 2021; accepted manuscript published online 14 May 2021; corrected proof published online 19 June 2021

STAT3, through its coiled–coil domain, is constitutively associated with the C-ter part of the IL-22Rα, devoid of Ys (Dumoutier et al., 2009).

Phosphotyrosine-dependent and -independent pathways cooperate to induce a massive activation of STAT3, which is involved in the vast majority of IL-22 functions. IL-22 displays beneficial effects because it promotes cell proliferation as well as antimicrobial peptide and chemokine production (Wolk et al., 2006). In colitis, IL-22 enables the regeneration of epithelium and defense against pathogens (Nagao-Kitamoto et al., 2020). Studies have shown that in the *Citrobacter rodentium*–induced model of colitis, *Il22*-deficient mice exhibit increased epithelial damage, submucosal inflammation, and colonic crypt bacteria penetration leading to more prominent weight loss and decreased survival rates compared with wild-type (WT) mice. This phenotype is associated with a reduction of antimicrobial protein expression (RegIIIβ, RegIIIγ, S100A8, and S100A9) crucial for the protective effect of IL-22 (Sugimoto et al., 2008; Zheng et al., 2008) as well as that of the fucosyltransferase *Fut2* (Pham et al., 2014). Nevertheless, in the case of an excess of IL-22, in an inflammatory environment, this cytokine becomes deleterious and has been described to be involved in diseases such as psoriasis (Boniface et al., 2005; Ma et al., 2008; Van Belle et al., 2012; van der Fits et al., 2009; Wolk et al., 2009; Zheng et al., 2007). First, *Il22*-transgenic mice present neonatal mortality and spontaneous typical psoriatic lesions (acanthosis and hyperkeratosis) (Wolk et al., 2009). Moreover, $Il22^{-/-}$ or anti–IL-22–blocking antibody–treated mice are partially protected against imiquimod-induced psoriasis-like dermatitis. Indeed, they exhibit reduced acanthosis, correlated with a decrease in neutrophils along with chemokines and keratinocyte differentiation gene expression (Van Belle et al., 2012). Protection of these mice is also observed in other skin inflammatory models such as IL-23–induced acanthosis and adoptive transfer model (Ma et al., 2008; Zheng et al., 2007).

STAT3 was shown to play a considerable role in the development of psoriasis. Indeed, transgenic mice with the expression of a constitutively active STAT3 in the basal layer of keratinocytes (K5.*STAT3C* mice) develop skin lesions that mimic psoriasis, with hyperkeratosis, parakeratosis, defect in keratinocyte differentiation, and hyperproliferation. STAT3 is also hyperactivated in psoriatic plaques from patients (Sano et al., 2005). Moreover, the deleterious effects of IL-22 observed in psoriasis are mediated by STAT3 (Wolk et al., 2009). Therefore, preventing the alternative activation of IL-22 could be a targeted therapy in psoriasis. Such therapy might lead to decreased activation of STAT3, blocking the deleterious effects of IL-22 while leaving intact the beneficial ones. In this context, we investigated the implication of the C-ter part of IL-22Rα in vivo in IL-22 signaling and the development of IL-22–mediated inflammation. In this paper, we report that the alternative pathway plays a major role in IL-22 signaling in the skin and in the liver but only a minor part in the ileum. Mice deficient in *Il22ra1* or with a truncated receptor were partially protected from the imiquimod model. In contrast, only *Il22ra1*-deficient mice were sensitive to the colitis model induced by *C. rodentium*.

RESULTS

The C-ter part of IL-22Rα plays a major role in IL-22 signaling in the skin but only a minor role in the gut

To study the alternative activation of STAT3 in vivo, mice with a truncated IL-22 receptor were generated using the CRISPR/Cas9 approach. A STOP codon was inserted at position 500, nine residues after the last Y (Tyr491), generating ΔCter-mutant mice (Supplementary Figure S1a). This prevents the preassociation of STAT3 with this region, enabling us to establish its relevance in IL-22 signaling in vivo. Being that IL-22Rα is expressed in several organs, IL-22 signaling was investigated in the skin, gut, lungs, liver, and kidneys. Epidermal cells from ear skin were stimulated ex vivo, and we observed reduced phosphorylated STAT3 (pSTAT3) in the cells with a truncation of the C-ter part of IL-22Rα (from $\Delta Cter^{mut/mut}$ mice) compared with that of cells from littermate controls ($\Delta Cter^{wt/wt}$ mice) (Figure 1a and Supplementary Figure S1b). The induction of *Socs3*, a STAT3-dependent gene, was weaker in the epidermal cells from $\Delta Cter^{mut/mut}$ mice after IL-22 stimulation than in those from littermate controls (Figure 1b and c). Surprisingly,STAT5 phosphorylation was increased in the cells, possibly owing to a compensatory phenomenon, whereas Jak1, STAT1, and extracellular signal–regulated kinase phosphorylation remained stable (Figure 1a and Supplementary Figure S1b). Hence, in the epidermis, the truncation of IL-22Rα partially represses its activation of STAT3.

IL-22 response in other organs was analyzed after intraperitoneal injection of the cytokine. In the distal ileum and the colon, pSTAT3 levels were similar in $\Delta Cter^{mut/mut}$ and $\Delta Cter^{wt/wt}$ mice (Figure 2a and Supplementary Figure S2a). These results were confirmed by pSTAT3 immunohistofluorescence on ileum sections (Figure 2b). Basal expression and induction of *Socs3* expression after IL-22 administration were also similar in $\Delta Cter^{mut/mut}$ and $\Delta Cter^{wt/wt}$ mice in both ileum and colon (Figure 2c–f). However, the basal expressions of *Reg3b* and *Fut2*, whose expressions are regulated by IL-22, were reduced in $\Delta Cter^{mut/mut}$ mice as compared with WT mice (Figure 2c). Interestingly, the level of induction (by exogenously administered IL-22) of these genes was similar between $\Delta Cter^{mut/mut}$ and $\Delta Cter^{wt/wt}$ mice in the ileum as well as in the colon (Figure 2e and Supplementary Figure S2b). These results suggest that the alternative pathway plays a role in the presence of physiological levels of IL-22 in the gut but not after the injection of exogenous IL-22. In other organs (liver, lungs, and kidneys), the induction of *Socs3* expression after IL-22 injection was reduced in mutant mice compared with that in the WT mice (Figure 3a–f). The expression of *Saa1-2* in the liver was also impacted by the C-ter part deletion (Figure 3a and d). It correlated with a strong decrease of STAT3 phosphorylation in the liver of $\Delta Cter^{mut/mut}$ mice compared with that in the WT mice (Figure 3g). Of note, IL-22Rα expression, at the RNA and protein levels, was similar if not increased in $\Delta Cter^{mut/mut}$ mice compared with that in the littermate controls (Supplementary Figure S3a and b). Taking together, these data demonstrate that the C-ter part of IL-22Rα plays an important role in IL-22 signaling and, more particularly, in STAT3 activation in vivo as well. However, the level of involvement of the alternative pathway seems to be organ

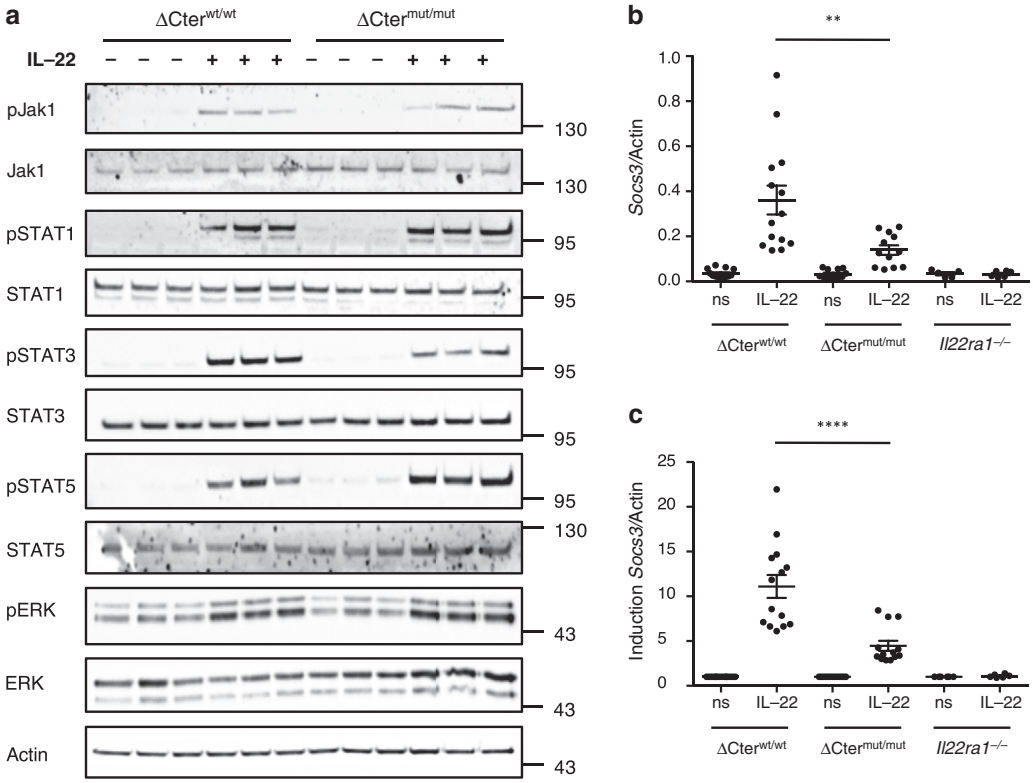

Figure 1. The C-ter part of IL-22Rα is involved in IL-22 signaling in the skin. (**a**) Western blot analysis of IL-22 signaling in epidermal cells. Epidermal cells from ΔCter$^{mut/mut}$ and WT littermate mice were stimulated ex vivo for 15 minutes with control medium or IL-22 (500 ng/ml) and lysed in NP40 lysis buffer. Total protein lysates were analyzed by western blot using antibodies directed against total or pSTAT1, pSTAT3, and pSTAT5, and pERK. The membranes were then reprobed with an anti–β-actin antibody. Blots are representative of four independent experiments (n = 3 mice per group in each experiment). (**b, c**) *Socs3* gene expression was analyzed by RT-qPCR in epidermal cells stimulated or not with IL-22 (500 ng/ml) for 60 minutes. *Socs3* gene expression is normalized against β-actin gene. In **c**, data are presented as induction compared with PBS injection. Data are shown as mean ± SEM and are pooled from three independent experiments (n = 3–5 mice per group in each experiment). Statistical analyses: Mann–Whitney (**$P < 0.01$ and ****$P < 0.0001$). C-ter, C-terminal; ERK, extracellular signal–regulated kinase; IL-22Rα, IL-22 receptor alpha; ns, not significant; pERK, phosphorylated extracellular signal–regulated kinase; pJak1, phopshorylated Jak1; pSTAT, phosphorylated signal transducer and activator of transcription; STAT, signal transducer and activator of transcription; WT, wild type.

specific. Hence, this region could turn out to be crucial in IL-22–dependent inflammatory models.

Deficiency and truncation of IL-22Rα dampens imiquimod-induced skin lesions

First, we took advantage of the imiquimod-induced psoriasis-like dermatitis model to define the role of IL-22Rα and its alternative activation of STAT3 in skin inflammation. Indeed, both IL-22 and STAT3 are known to be deleterious in this model. Mice were treated for 7 consecutive days with Aldara (Saint Paul, MN), and several parameters were analyzed and compared between B6 and *Il22ra1*$^{-/-}$ or ΔCter$^{wt/wt}$ and ΔCter$^{mut/mut}$ mice. As shown in Figure 4a, *Il22ra1*$^{-/-}$ mice were protected from ear thickening compared with B6 mice. ΔCter$^{mut/mut}$ mice also displayed significantly reduced ear thickening compared with WT littermates (Figure 4a) even if this protection seems less important than in *Il22ra1*$^{-/-}$ mice. The protection of both *Il22ra1*$^{-/-}$ and ΔCter$^{mut/mut}$ mice was also observed by histologically measuring the thickness of the epidermis and the number of crusts and pustules along with the tissue (Figure 4b, c, and d). As shown in a previous study, several genes were upregulated in this model in an IL-22–dependent manner, notably *Cxcl3* and *S100a8* (Van Belle et al., 2012). Both genes were significantly less induced in *Il22ra1*$^{-/-}$ and ΔCter$^{mut/mut}$ mice than in WT mice after imiquimod treatment (Figure 4e and f). Finally, the decrease of *Cxcl3* expression correlated with the decrease of neutrophils in the epidermis and dermis (Figure 4g and h). It is noteworthy that the *Il22ra1*$^{-/-}$ mice were more protected than the ΔCter$^{mut/mut}$ mice, suggesting that the alternative activation of STAT3 is responsible for a part of IL-22 signaling and function in this model. We conclude that the alternative pathway of STAT3 activation plays a role in IL-22–dependent skin inflammation.

Y-dependent activation of STAT3 by IL-22Rα is sufficient to protect mice from the weight loss induced by *C. rodentium* infection even if the C-ter region is required for *Reg3* expression

In parallel with skin inflammation, the impact of the IL-22Rα and its alternative pathway was also investigated in the gut using the *C. rodentium*–induced colitis model. After *C. rodentium* infection, mouse weight was followed for 2 weeks. From day 7 after bacterial infection, *Il22ra1*$^{-/-}$ and anti–IL-22Rα–treated B6 mice began to lose weight similarly, demonstrating the protective impact of IL-22 in this model (Figure 5a). In contrast, neither ΔCter$^{mut/mut}$ nor ΔCter$^{wt/wt}$ mice presented significant weight loss,

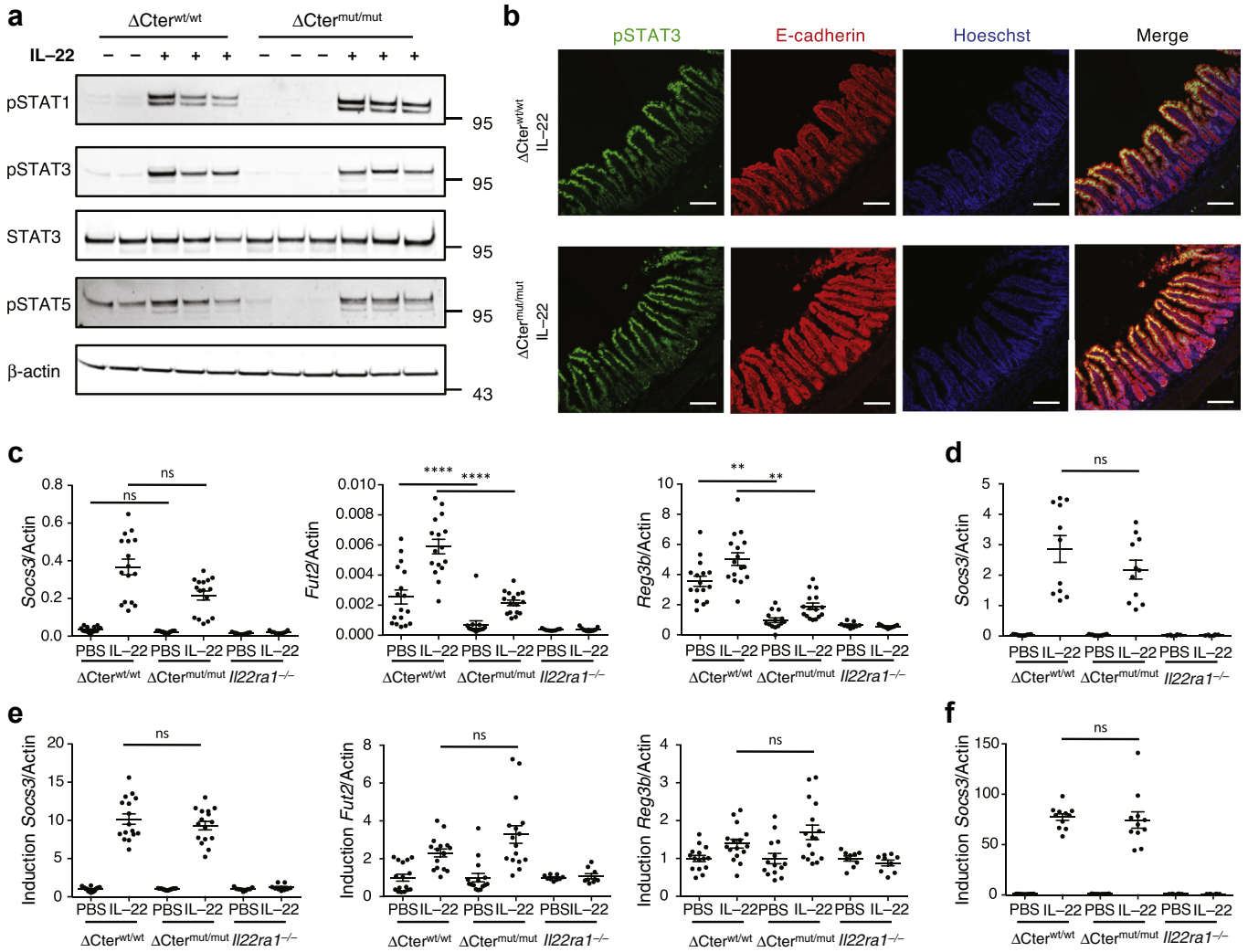

Figure 2. The C-ter part of IL-22Rα does not play a major role in IL-22 activities in the gut. ΔCter$^{mut/mut}$ mice and control littermate mice were treated intraperitoneally with PBS or IL-22 for 30 minutes (in **a** and **b**) or for 1 hour (in **c**–**f**). (**a**) Western blot analysis of IL-22 signaling in the ileum. Total protein lysates from the distal ileum were analyzed by western blot using antibodies directed against total or pSTAT1, pSTAT3, and pSTAT5. The membranes were then reprobed with an anti–β-actin antibody. Blots are representative of three independent experiments (n = 3 mice per group in each experiment). (**b**) Immunohistofluorescent staining on the frozen section of the ileum. Slides were stained for pSTAT3, E-cadherin, and Hoechst. Pictures are representative of two experiments. Bar = 100 μm. Original magnification = ×20. (**c, e**) Ileum and (**d, f**) colon were analyzed by RT-qPCR. One hour after PBS or IL-22 injection, organs were dissected, and RNA was extracted. *Socs3*, *Fut2*, and *Reg3g* gene expressions are normalized against that of β-actin gene. In **e** and **f**, data are presented as induction compared with PBS injection. Data are shown as mean ± SEM and are pooled from two or three independent experiments (n = at least 5 mice per group in each experiment). Statistical analyses: Kruskal–Wallis for **c**, Mann–Whitney for **d**–**f** (**$P < 0.01$ and ****$P < 0.0001$). C-ter, C-terminal; IL-22Rα, IL-22 receptor alpha; ns, not significant; pSTAT, phosphorylated signal transducer and activator of transcription; STAT, signal transducer and activator of transcription.

suggesting that the loss of the C-ter part does not prevent IL-22 signaling, consistent with western blot results obtained in the colon after IL-22 injection (Supplementary Figure S2a). However, the IL-22Rα–neutralizing antibody had a stronger effect on Δ*Cter*$^{mut/mut}$ than on the littermate controls (Figure 5a). This suggests that deletion of IL-22Rα C-ter part slightly decreases IL-22 responses in the gut, with only minor effects on *C. rodentium* infection, but can synergize with an anti–IL-22Rα antibody to aggravate the infection. At the histological level, we could not detect major differences between the groups (Figure 5b and Supplementary Figure S4a and b) in terms of crypt length and the presence of goblet cells, even though *Il22ra1*$^{-/-}$ and anti–IL-22Rα–treated mice tended to have fewer goblet cells. The expression of *Gob5*, a marker of goblet cells, in the colon was also decreased after anti–IL-22Rα treatment in the WT mice (Figure 5c). Finally, *Reg3g*, *Reg3b*, and *Fut2* were less expressed in *Il22ra1*$^{-/-}$ and ΔCter$^{mut/mut}$ mice than in the WT mice. Similarly, IL-22Rα–neutralizing treatment significantly reduced their expression in the WT mice but not in the mutant mice (Figure 5d and e and Supplementary Figure S4c). We conclude that *Il22ra1* is essential to protect mice against the *C. rodentium* model. In contrast, although some parameters were reduced, ΔCter$^{mut/mut}$ mice did not lose significantly more weight than their WT counterparts. Hence, the absence of an alternative pathway does not prevent the beneficial impact of IL-22 after *C. rodentium* infection, meaning that the Y-dependent pathway is sufficient to mediate protective STAT3 activation.

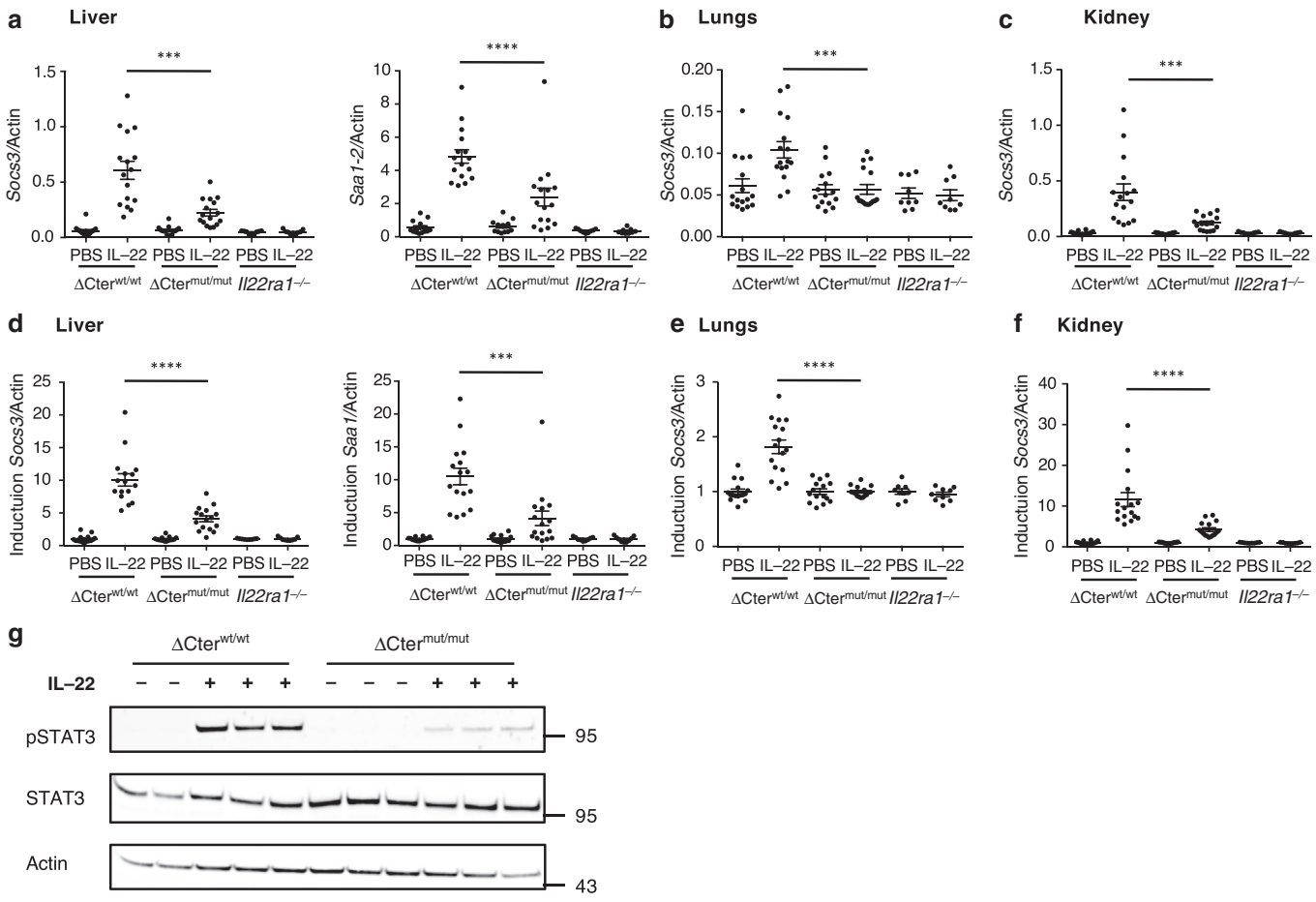

Figure 3. The C-ter part of IL-22Rα is involved in IL-22 response in the liver, lungs, and kidney. (**a**–**f**) RNA was extracted from (**a**, **d**) liver, (**b**, **e**) lungs, and (**c**, **f**) kidney 1 hour after PBS or IL-22 injection. RT-qPCR was performed for *Socs3* and *Saa1-2*. Results were normalized to β-actin gene. In **d**–**f**, data are presented as induction compared with PBS injection. Data are shown as mean ± SEM and are pooled from three independent experiments (n = at least 5 mice per group in each experiment). Statistical analyses: Mann–Whitney (***$P < 0.001$ and ****$P < 0.0001$). (**g**) Western blot analysis of IL-22 signaling in the liver. At 30 minutes after PBS or IL-22 intraperitoneal injection, a piece of liver was cut and frozen. Proteins were extracted, and 2 μg of proteins was charged on gels. STAT3 and pSTAT3 were analyzed. C-ter, C-terminal; IL-22Rα, IL-22 receptor alpha; pSTAT, phosphorylated signal transducer and activator of transcription; STAT, signal transducer and activator of transcription.

DISCUSSION

Our study confirms that IL-22 is involved in skin and gut inflammation. Indeed, as previously described in *Il22*$^{-/-}$ mice (Van Belle et al., 2012), *Il22ra1*-deficient mice were partially protected in the imiquimod model and were sensitive to the *C. rodentium* model. Our results also indicate that the C-ter part of IL-22Rα is involved in the activation of STAT3 but not of STAT1 or STAT5 in vitro and in vivo. These results are consistent with our previous study showing this alternative activation of STAT3 in BW5147 mice engineered to express mutant forms of IL-22Rα (Dumoutier et al., 2009). In addition, we show that this alternative activation of STAT3 is deleterious in the imiquimod-induced psoriasis-like dermatitis model, whereas its role in the *C. rodentium*–induced colitis is limited.

Alternatively, receptor Y-independent activation of STAT has been described for IL-22Rα and IFN-λ receptor, both receptors that bind cytokines of the IL-10 family. Therefore, we may wonder whether all cytokines of this family can activate an alternative pathway. Two Ys of IL-10 receptor alpha were shown to be required for STAT3 activation, making the alternative activation of STAT3 by IL-10 unlikely (Weber-Nordt et al., 1996). Y-independent modes of STAT activation have also been described for cytokine receptors unrelated to the IL-10R family, including IFNAR, G-CSF-R, and IL-23 receptor (Dumoutier et al., 2004; Floss et al., 2013; Li et al., 1997; Nicholson et al., 1996; Ward et al., 1999). These alternative pathways enable massive activation of STAT signaling, and the preassociation of STAT with the receptor may also allow for faster responses to cytokine stimulation. However, data on their biological relevance are still missing. Our study shows the role of such an alternative pathway in a physiological context in vitro and in vivo.

In the imiquimod model, ΔCter$^{mut/mut}$ mice displayed milder acanthosis than ΔCter$^{wt/wt}$ mice. This was accompanied by reduced expression of *S100a8* and *Cxcl3,* correlating with a smaller percentage of neutrophils in the dermis and the epidermis. The partial protection of ΔCter$^{mut/mut}$ mice from the imiquimod model was weaker than the one observed for *Il22ra1*$^{-/-}$ mice, suggesting that the Y-independent activation of STAT3 is partially involved

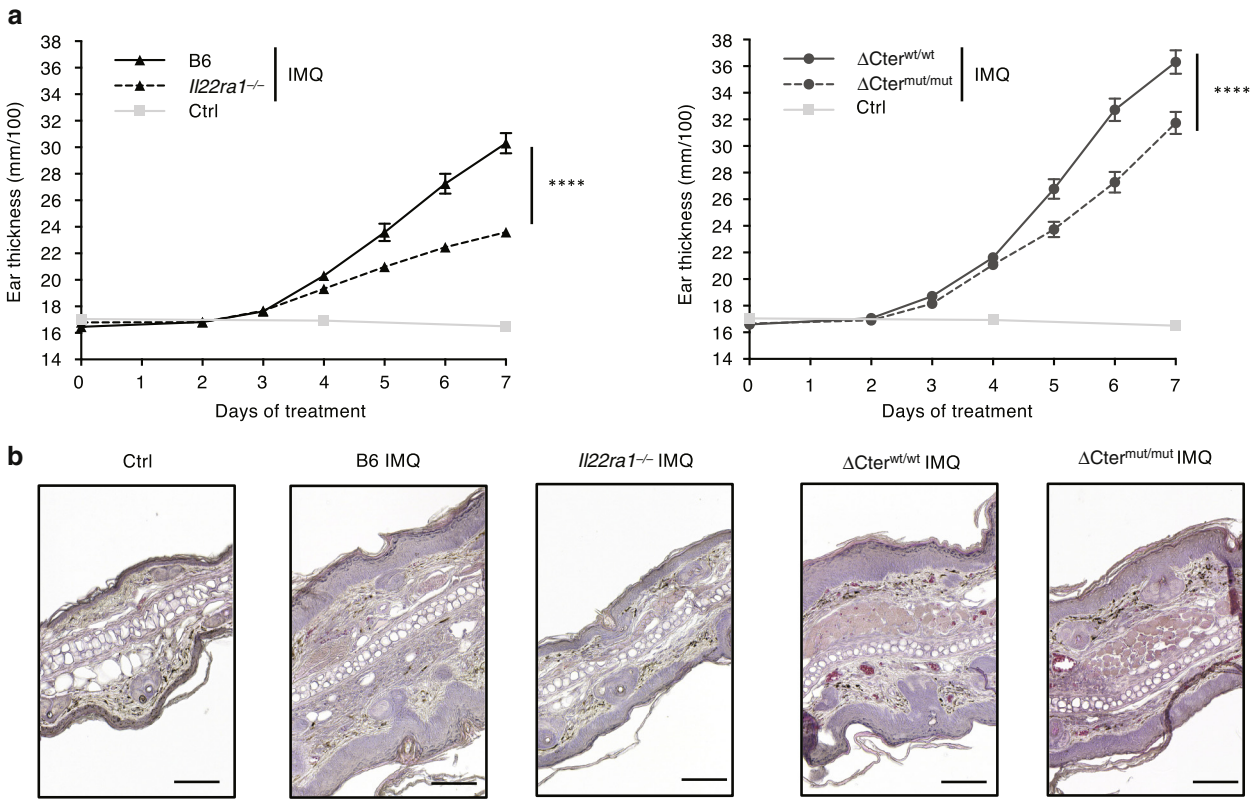

Figure 4. Deficiency and truncation in IL-22Rα protect in the imiquimod-induced psoriasis-like dermatitis model. (**a–h**) B6, *Il22ra1*$^{-/-}$, ΔCter$^{wt/wt}$, and ΔCter$^{mut/mut}$ mice were treated daily with imiquimod on the ears for 7 days. Data are shown as mean ± SEM and are pooled from three independent experiments (n = 8 mice per group in each experiment). (**a**) Ear thickness was measured daily with a micrometer screw to evaluate acanthosis. (**b**) H&E staining of ear sections. Bar = 100 μm; original magnification = ×20. One representative picture is shown for each group. (**c**) Acanthosis was evaluated by measuring the epidermal thickness at a minimum of 20 different places using Panoramic viewer software. (**d**) The numbers of crusts and pustules divided by the length of the skin sections are represented. (**e, f**) RT-qPCR was performed for *Cxcl3* and *S100a8*. Results were normalized to β-actin gene. (**g, h**) Flow cytometry analysis of neutrophils in the (**g**) epidermis and (**h**) dermis. Cells were gated on live CD45^{+} cells, and neutrophils were analyzed using Ly6G and CD11b markers. Statistical analyses: (**a**) two-way ANOVA with Bonferroni posthoc test; (**c**—**h**) Mann–Whitney (*$P < 0.05$, ***$P < 0.001$ and ****$P < 0.0001$). Ctrl, control; IL-22Rα, IL-22 receptor alpha; IMQ, imiquimod; ns, not significant.

in IL-22 signaling and effects in the skin. However, it seems that IL-22Rα was more expressed in the ΔCter$^{mut/mut}$ than in the ΔCter$^{wt/wt}$ mouse epidermal cells (Supplementary Figure S2a). Hence, the effect of the IL-22Rα C-ter part on STAT3 activation might be underestimated.

Strikingly, the effects of the truncation of IL-22Rα on *C. rodentium* infection or STAT3 signaling in the gut is very limited compared with that in the skin and liver, where STAT3 activation is strongly decreased in ΔCter$^{mut/mut}$ mice. This is not due to changes in STAT3 or IL-22Rα expression in the gut that may modify the unconventional association between these two partners (Supplementary Figure S3a and b; data not shown). The impact of the C-ter part might be different depending on the cell type and the presence of intermediate proteins required for this interaction, with low expression in the gut potentially accounting for these differences. However, the preassociation of STAT3 with IL-22Rα was detected in HT-29 and Colo205, two epithelial cell lines derived from colorectal cancer, suggesting that the alternative pathway can take place in the gut (Dumoutier et al., 2009). Nonetheless, these are cells in culture that do not fully reflect the in vivo physiological context where environmental factors (such as microbiota) may influence the expression of such intermediate proteins.

The alternative activation of STAT3 has a deleterious effect in the imiquimod model, making it a promising therapeutic target. Currently, treatments used in patients with psoriasis include topical treatment and psoralens plus UVA therapy for mild forms and anti-inflammatory or immunosuppressive molecules such as corticosteroids, cyclosporin, and methotrexate for more severe forms. Over the last two decades, the use of biologics targeting TNF-α, IL-23, or IL-17 has greatly improved the treatment of psoriasis (Martins et al., 2020), leading to a 90% reduction of the PASI score in a large proportion of patients (Ghoreschi et al., 2021). However, some patients do not respond to such therapy or develop side effects such as upper respiratory tract infections, headache, mild neutropenia, candidiasis, and less commonly, worsening of inflammatory bowel disease (Ghoreschi et al., 2021). These side effects are most probably due to the broad impact of these biologics on the immune system. Given that IL-22Rα is not expressed by immune cells, targeting IL-22 signaling may be advantageous because it would not affect the immune system. Moreover, specifically targeting the alternative activation of

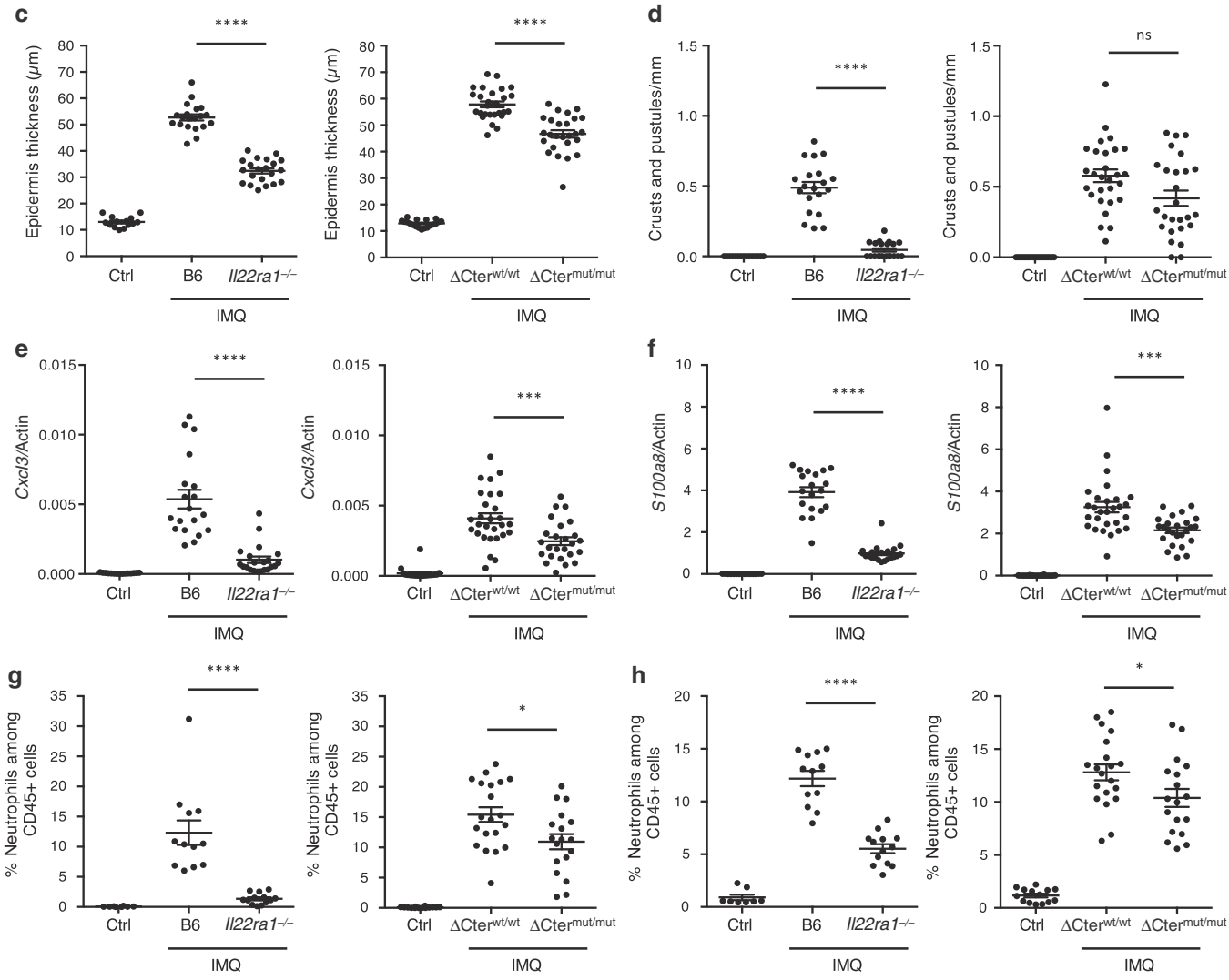

Figure 4. (*continued*).

STAT3 would enable the partial decrease of IL-22 signaling, dampening its harmful effects in psoriasis, while maintaining its beneficial effects in contexts such as colitis. C-ter part–dependent activation of STAT3 has also been demonstrated in the human cell line A549 (data not shown), showing that this mechanism also exists in humans. Small molecules or binding proteins such as monobodies could be used to perturb the preassociation of STAT3 with the C-ter part of IL-22Rα (Sha et al., 2017).

MATERIALS AND METHODS

Mice and reagents

All mice used in this study were bred in our animal facility under specific pathogen-free conditions. *Il22ra1*$^{-/-}$ mice were generated in 129sv/C57BL/6 background in our laboratory as previously described (Van Belle et al., 2019). Mice were backcrossed 20 times on C57BL/6, allowing us to use C57BL/6 of our animal facilities as controls (called B6 thereafter). To generate ΔCter$^{mut/mut}$ mice, we used a cloning-free CRISPR/Cas9 system to target the mouse *Il22ra1* gene (Aida et al., 2015). Guide RNA is split in two: CRISPR RNA (crRNA) (20 nucleotides), corresponding to the target sequence with a tail (16 nucleotides), and a trans-activating CRISPR RNA (tracrRNA) (67 nucleotides), containing the hairpin recognized by Cas9 with an extremity complementary to the crRNA tail. Recombinant Cas9 protein, annealed crRNA/tracrRNA, and single-strand DNA donor (2.4 pmol/μl crRNA, 2.4 pmol/μl tracrRNA, 100 ng/μl Cas9, and 10 ng/μl single-strand DNA donor) were mixed in Integrated DNA Technology buffer, that is, 10 mM Tris, 0.1 mM EDTA buffer, and injected into the pronucleus of B6D2 mouse zygotes. crRNA, tracrRNA, single-strand DNA donor, and recombinant Cas9 protein were purchased from Integrated DNA Technologies (Leuven, Belgium). Sequences of guide RNA and single-strand DNA are provided in the Supplementary Table S1. The presence of the mutation in pups was confirmed by PCR screening and sequencing. Mice carrying the mutation were crossed with C57BL/6 female, and the strain was kept in a littermate background (B6D2x C57BL/6). ΔCter$^{wt/wt}$ mice were used as a control of ΔCter$^{mut/mut}$ mice. Mice were selected on the basis of the presence of the mutation in the *Il22ra1* by PCR genotyping.

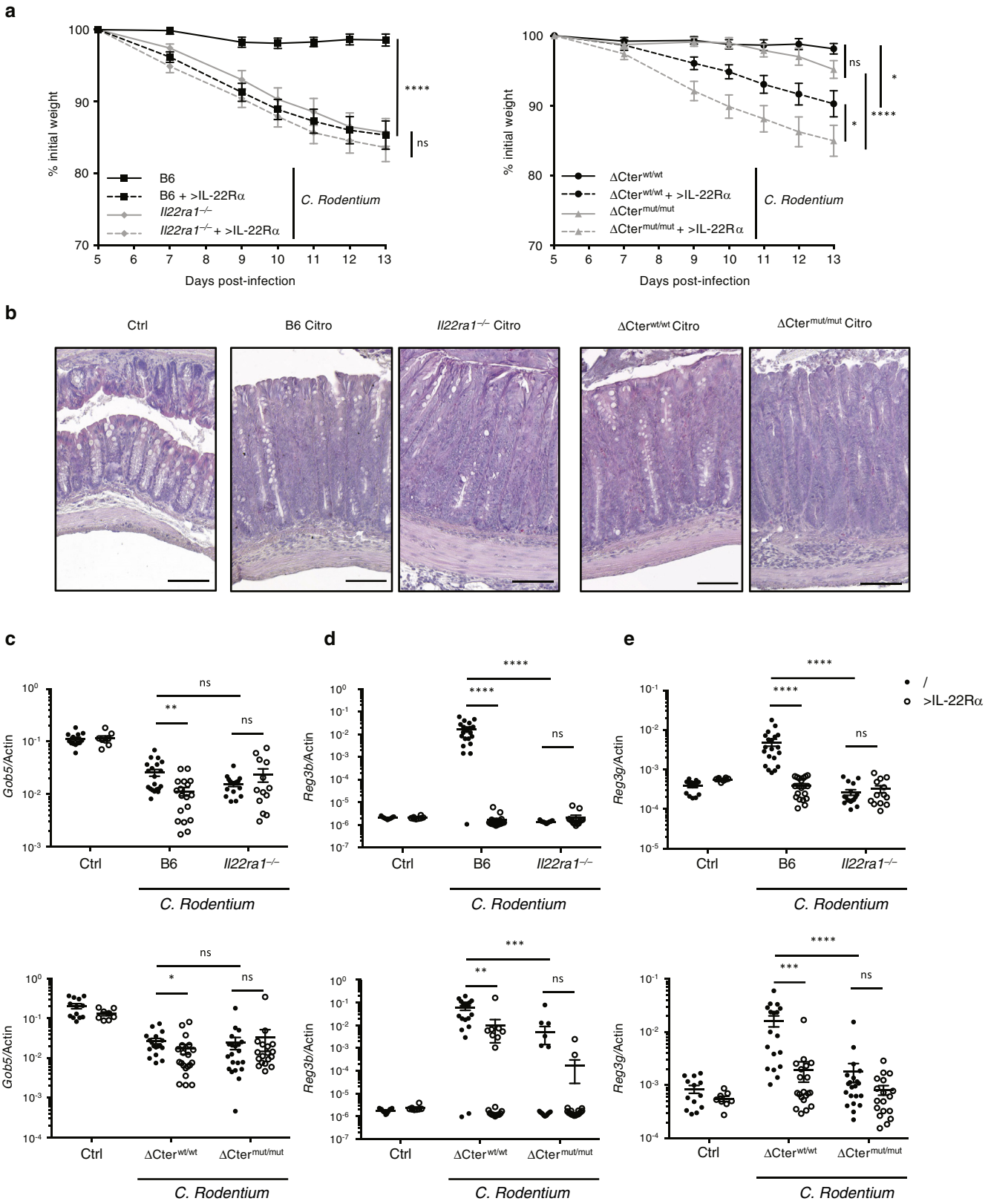

Figure 5. IL-22Rα C-ter part has only a minor role in *C. rodentium*–induced colitis. (**a**–**e**) Mice were orally infected with 2 × 10^9 CFU of *C. rodentium* and intraperitoneally injected with anti–IL-22Rα antibodies (>IL-22Rα, 100 μg/mice) 1 d before gavage and each 3 to 4 d (d2, d5, d9). Data are shown as mean ± SEM and are pooled from three independent experiments (n = min 6 mice per group in each experiment). (**a**) Bodyweight was measured to evaluate the colitis. (**b**) H&E staining of colon sections. Bar = 100 μm; original magnification = ×20. One representative picture is shown for each group. (**c**–**e**) RNA was extracted from the colon, and RT-qPCR was performed for *Gob5*, *Reg3b*, and *Reg3g*. Results were normalized to that of β-actin gene. Statistical analyses: (**a**) two-way ANOVA with Bonferroni posthoc test; (**c**–**e**) Kruskal–Wallis (*$P < 0.05$, **$P < 0.01$, ***$P < 0.001$ and ****$P < 0.0001$). CFU, colony-forming unit; C-ter, C-terminal; Ctrl, control; d, day; IL-22Rα, IL-22 receptor alpha; ns, not significant.

All mouse experiments were performed in compliance with national and institutional guidelines and were approved by the local ethical committee (LA 1230653-2019/UCL/MD/021 and 2019/UCL/MD/022).

Anti–IL-22Rα antibody was obtained by subcloning the VH (280-VH3-66.46) and VKappa (VK4-1-TSY) from patent US_8545844 into a human IgG1 backbone effector function dead (E233P, L234V, L235A). Recombinant mouse IL-22 was produced in *E. coli* as described previously (Dumoutier et al., 2000b).

Imiquimod model

Mice aged 8 weeks were shaved behind the ears and were treated with seven daily topical applications of imiquimod (0.8 mg per ear) from a commercially available cream (Aldara 5%; 3M). Ear thickness was measured every day with a micrometer screw (Mitutoyo, Kawasaki, Japan). After 7 days, mice were killed: one ear was used for H&E staining, whereas the other was used for RNA extraction and the epidermis or dermis single-cell purification followed by FACS staining as previously described (Cochez et al., 2017). Western blot and RT-qPCR on epidermal cell suspension were performed after 24 hours at 37 ° in wells (48 wells plate).

C. rodentium infection

C. rodentium infection was made with the strain DBS100 (kindly provided by M. Chamaillard, Pasteur Institute, Lille, France). Six colonies were cultured for 4 hours in 5 ml Luria Bertani media. Then, 350 ml of Luria Bertani was added, and bacteria were cultured overnight. The bacteria were centrifuged, washed, resuspended in PBS, and adjusted to 10^{10} colony-forming unit/ml of *C. rodentium*. Mice aged 8 weeks were orally infected with a 2×10^9 colony-forming unit of *C. rodentium*. To monitor the infection, the body weight was measured frequently. Anti–IL-22Rα antibody (100 μg/mice) was injected in half of the mice 1 day before gavage and on day 2, day 5, and day 9 after infection. Mice were killed 13 days after infection; one part of the distal colon was used for the histology, and a second segment was frozen after incubation in RNAlater (Thermo Fisher Scientific, Waltham, MA) until RNA extraction.

Intestinal single-cell suspension

Intestines were dissected and cut longitudinally after removing the Peyer's patches and the fat. Small pieces of intestines were incubated with EDTA (2.5 mM) and dithiothreitol (72.5 mg/ml) for 20 minutes at 37 °C with shaking (200 r.p.m.). After mechanical disruption, cells were passed through a 70-mm cell strainer and were further centrifuged in a solution of 30% Percoll. FACS analyzes were directly performed on epithelial cells.

FACS staining

Cells were preincubated with 10 μg/ml of purified rat anti-mouse CD16–CD32 mAb (Fc Block; BD Biosciences, San Jose, CA) before incubation with a viability marker (LIVE/DEAD Fixable Near-IR Dead Cell Stain Kit, Life Technologies, Carlsbad, CA) and 2 μg/ml of antibodies to extracellular staining for 30 minutes at 4 °C. Then, for intracellular staining, cells were fixed, permeabilized using the Intracellular Fixation & Permeabilization Buffer Set (Thermo Fisher Scientific), and finally stained for 30 minutes at 4 °C. Cells were analyzed with a FACS Fortessa (BD Biosciences). The commercial antibodies used in this study are provided in Supplementary Table S2. Anti–IL-22Rα (AM22R1.1) is unlabeled and is produced in our laboratory. This IL-22Rα staining requires a bilayer staining with, as the second layer, the PE Goat anti-mouse IgG antibody (405307, Biolegend, San Diego, CA).

The gating strategy included forward and side scatter, a viability marker, and CD45 expression. Cytokeratin 10 and epithelial cell adhesion molecule markers allow discrimination of keratinocytes and intestinal epithelial cells, respectively (Supplementary Figure S5a). Ly6G and CD11b markers were used to analyze neutrophils (Supplementary Figure S5b). The specificity of the IL-22Rα staining was verified in *Il22ra1*$^{-/-}$ mice. Data were analyzed with the FlowJo software (Tree Star, Ashland, OR).

Western blot

Cells were stimulated for 15 minutes at 37 °C with a control medium or with murine IL-22 (500 ng/ml). For mice, IL-22 was intraperitoneally injected, and after 30 minutes, organs were frozen in liquid nitrogen before tissue disruption with TissueLyser LT (Qiagen, Hilden, Germany). Lysis was performed as previously described (Springuel et al., 2014). After protein quantification with Pierce BCA Protein Assay Kit (Thermo Fisher Scientific), a total of 2 or 10 μg of proteins diluted in LDS sample buffer and Sample Reducing Agent (Thermo Fisher Scientific) were loaded on Bolt 4–12% Bis-tris gels (Thermo Fisher Scientific) and transferred to nitrocellulose membrane (iBlot Gel Transfer Stacks, Thermo Fisher Scientific). The Jak–STAT signaling pathway was investigated with the antibodies provided in Supplementary Table S2.

RT-qPCR

IL-22 (10 μg) was injected intraperitoneally, and different organs were dissected 1 hour after injection. After 24 hours in RNAlater (Thermo Fisher Scientific), total RNA was isolated from organs with the TriPure Isolation Reagent (Roche, Basel, Switzerland) after tissue disruption with TissueLyser LT (Qiagen). RNA extraction from cells was performed 1 hour after stimulation with control medium or with murine IL-22 (500 ng/ml) and also with TriPure Isolation Reagent. RT-qPCR was performed as previously described (Cochez et al., 2017). The sequences of primers and probes are provided in Supplementary Table S3.

Histology and immunohistofluorescence

Paraffin embedding of ears or intestine was performed using routine methods. Sections that were 6 μm in length were stained with H&E and scanned with Pannoramic 250 (3DHISTECH, Budapest, Hungary).

Intestines were dissected, cut longitudinally, and washed briefly in PBS before fixation in paraformaldehyde 4% for 30 minutes at 4 °C. Organs were then embedded in 15% sucrose/7.5% gelatin and were frozen. Immunofluorescence labeling was performed on 10 μm tissue sections after antigen unmaking in a citrate buffer (0.01 M, pH 6.0). The following antibody allowed to study pY705 STAT3 (#9145, dilution of 1/200, Cell Signaling Technology, Danvers, MA). Anti–E-cadherin antibody was used as an epithelial marker (#610181, dilution of 1/250, BD biosciences). Secondary antibodies AF488 Donkey anti-Rabbit IgG (A21206, Thermo Fisher Scientific) and AF594 Donkey anti-Rabbit IgG (A21207, Thermo Fisher Scientific) as well as Hoechst (Sigma-Aldrich, St. Louis, MO) were applied at 1/1,000. Slides were scanned with Pannoramic 250 (3DHISTECH).

Statistics

Results are presented as the mean ± SEM, and statistical analyses were performed using the Prism software (GraphPad Software, La Jolla, CA). Statistical significance between groups of WT and *Il22ra1*$^{-/-}$ or ΔCter$^{mut/mut}$ mice was assessed with the Mann–

Whitney test (nonparametric conditions). When we compared >2 groups, statistical significance was assessed by the Kruskal–Wallis test, followed by Dunn's multiple comparisons posthoc test. Two-way ANOVA with Bonferroni posthoc test was used for the ear thickening and weight loss curves.

Data availability statement

No datasets were generated or analyzed during this study.

ORCIDs

Camille Michiels: https://orcid.org/0000-0002-5173-5555
Léna Puigdevall: https://orcid.org/0000-0002-5451-6673
Perrine Cochez: https://orcid.org/0000-0002-2721-6675
Younes Achouri: https://orcid.org/0000-0001-7409-1441
Paméla Cheou: https://orcid.org/0000-0001-8368-4740
Emilie Hendrickx: https://orcid.org/0000-0002-6765-2711
Nicolas Dauguet: https://orcid.org/0000-0002-4416-9903
Christophe Blanchetot: https://orcid.org/0000-0001-9152-9978
Laure Dumoutier: https://orcid.org/0000-0002-6645-684X

CONFLICT OF INTEREST

The authors state no conflict of interest.

ACKNOWLEDGMENTS

This work was supported by the Actions de Recherche Concertées of the Communauté Française de Belgique and the Fonds National de la Recherche Scientifique. LD is a senior research associate with the Fonds National de la Recherche Scientifique, Belgium. CM and PCh were supported by the Actions de Recherche Concertées of the Communauté Française de Belgique, and CM have been granted with a Fund for Research training in Industry and Agriculture. We are very grateful to N. Limaye for her editing assistance.

AUTHOR CONTRIBUTIONS

Conceptualization: CM, LD; Data Curation: CM, LP, LD; Formal Analysis: CM, LP, LD; Funding Acquisition: LD; Investigation: CM, PCh, LP, PCo, EH, ND; Methodology: CM, PCh, LP; Project Administration: CM, LD; Resources: CM, YA, ND, CB; Supervision: LD; Validation: CM, LD; Visualization: CM, LD; Writing - Original Draft Preparation: CM, LD; Writing - Review and Editing: CM, PCh, LP, PCo, EH, ND, YA, CB, LD

SUPPLEMENTARY MATERIAL

Supplementary material is linked to the online version of the paper at www.jidonline.org, and at https://doi.org/10.1016/j.jid.2021.04.016.

REFERENCES

Aida T, Chiyo K, Usami T, Ishikubo H, Imahashi R, Wada Y, et al. Cloning-free CRISPR/Cas system facilitates functional cassette knock-in in mice. Genome Biol 2015;16:87.

Boniface K, Bernard FX, Garcia M, Gurney AL, Lecron JC, Morel F. IL-22 inhibits epidermal differentiation and induces proinflammatory gene expression and migration of human keratinocytes. J Immunol 2005;174:3695–702.

Cochez PM, Michiels C, Hendrickx E, Dauguet N, Warnier G, Renauld JC, et al. CCR6 is dispensable for the development of skin lesions induced by imiquimod despite its effect on epidermal homing of IL-22-producing cells. J Invest Dermatol 2017;137:1094–103.

Dumoutier L, de Meester C, Tavernier J, Renauld JC. New activation modus of STAT3: a tyrosine-less region of the interleukin-22 receptor recruits STAT3 by interacting with its coiled-coil domain. J Biol Chem 2009;284:26377–84.

Dumoutier L, Louahed J, Renauld JC. Cloning and characterization of IL-10-related T cell-derived inducible factor (IL-TIF), a novel cytokine structurally related to IL-10 and inducible by IL-9. J Immunol 2000a;164:1814–9.

Dumoutier L, Tounsi A, Michiels T, Sommereyns C, Kotenko SV, Renauld JC. Role of the interleukin (IL)-28 receptor tyrosine residues for antiviral and antiproliferative activity of IL-29/interferon-lambda 1: similarities with type I interferon signaling. J Biol Chem 2004;279:32269–74.

Dumoutier L, Van Roost E, Colau D, Renauld JC. Human interleukin-10-related T cell-derived inducible factor: molecular cloning and functional characterization as an hepatocyte-stimulating factor. Proc Natl Acad Sci USA 2000b;97:10144–9.

Floss DM, Mrotzek S, Klöcker T, Schröder J, Grötzinger J, Rose-John S, et al. Identification of canonical tyrosine-dependent and non-canonical tyrosine-independent STAT3 activation sites in the intracellular domain of the interleukin 23 receptor. J Biol Chem 2013;288:19386–400.

Ghoreschi K, Balato A, Enerbäck C, Sabat R. Therapeutics targeting the IL-23 and IL-17 pathway in psoriasis. Lancet 2021;397:754–66.

Kotenko SV, Izotova LS, Mirochnitchenko OV, Esterova E, Dickensheets H, Donnelly RP, et al. Identification of the functional interleukin-22 (IL-22) receptor complex: the IL-10R2 chain (IL-10Rbeta) is a common chain of both the IL-10 and IL-22 (IL-10-related T cell-derived inducible factor, IL-TIF) receptor complexes. J Biol Chem 2001;276:2725–32.

Lejeune D, Dumoutier L, Constantinescu S, Kruijer W, Schuringa JJ, Renauld JC. Interleukin-22 (IL-22) activates the JAK/STAT, ERK, JNK, and p38 MAP kinase pathways in a rat hepatoma cell line. Pathways that are shared with and distinct from IL-10. J Biol Chem 2002;277:33676–82.

Li X, Leung S, Kerr IM, Stark GR. Functional subdomains of STAT2 required for preassociation with the alpha interferon receptor and for signaling. Mol Cell Biol 1997;17:2048–56.

Ma HL, Liang S, Li J, Napierata L, Brown T, Benoit S, et al. IL-22 is required for Th17 cell-mediated pathology in a mouse model of psoriasis-like skin inflammation. J Clin Invest 2008;118:597–607.

Martins AM, Ascenso A, Ribeiro HM, Marto J. Current and future therapies for psoriasis with a focus on serotonergic drugs. Mol Neurobiol 2020;57:2391–419.

Morris R, Kershaw NJ, Babon JJ. The molecular details of cytokine signaling via the JAK/STAT pathway. Protein Sci 2018;27:1984–2009.

Nagao-Kitamoto H, Leslie JL, Kitamoto S, Jin C, Thomsson KA, Gillilland MG 3rd, et al. Interleukin-22-mediated host glycosylation prevents Clostridioides difficile infection by modulating the metabolic activity of the gut microbiota. Nat Med 2020;26:608–17.

Nicholson SE, Starr R, Novak U, Hilton DJ, Layton JE. Tyrosine residues in the granulocyte colony-stimulating factor (G-CSF) receptor mediate G-CSF-induced differentiation of murine myeloid leukemic (M1) cells. J Biol Chem 1996;271:26947–53.

Pham TA, Clare S, Goulding D, Arasteh JM, Stares MD, Browne HP, et al. Epithelial IL-22RA1-mediated fucosylation promotes intestinal colonization resistance to an opportunistic pathogen. Cell Host Microbe 2014;16:504–16.

Sabat R, Ouyang W, Wolk K. Therapeutic opportunities of the IL-22-IL-22R1 system. Nat Rev Drug Discov 2014;13:21–38.

Sano S, Chan KS, Carbajal S, Clifford J, Peavey M, Kiguchi K, et al. Stat3 links activated keratinocytes and immunocytes required for development of psoriasis in a novel transgenic mouse model. Nat Med 2005;11:43–9.

Sha F, Salzman G, Gupta A, Koide S. Monobodies and other synthetic binding proteins for expanding protein science. Protein Sci 2017;26:910–24.

Springuel L, Hornakova T, Losdyck E, Lambert F, Leroy E, Constantinescu SN, et al. Cooperating JAK1 and JAK3 mutants increase resistance to JAK inhibitors. Blood 2014;124:3924–31.

Sugimoto K, Ogawa A, Mizoguchi E, Shimomura Y, Andoh A, Bhan AK, et al. IL-22 ameliorates intestinal inflammation in a mouse model of ulcerative colitis. J Clin Invest 2008;118:534–44.

Tian SS, Tapley P, Sincich C, Stein RB, Rosen J, Lamb P. Multiple signaling pathways induced by granulocyte colony-stimulating factor involving activation of JAKs, STAT5, and/or STAT3 are required for regulation of three distinct classes of immediate early genes. Blood 1996;88:4435–44.

Van Belle AB, Cochez PM, de Heusch M, Pointner L, Opsomer R, Raynaud P, et al. IL-24 contributes to skin inflammation in para-phenylenediamine-induced contact hypersensitivity. Sci Rep 2019;9:1852.

Van Belle AB, de Heusch M, Lemaire MM, Hendrickx E, Warnier G, Dunussi-Joannopoulos K, et al. IL-22 is required for imiquimod-induced psoriasiform skin inflammation in mice. J Immunol 2012;188:462–9.

van der Fits L, Mourits S, Voerman JS, Kant M, Boon L, Laman JD, et al. Imiquimod-induced psoriasis-like skin inflammation in mice is mediated via the IL-23/IL-17 axis. J Immunol 2009;182:5836–45.

Ward AC, Hermans MH, Smith L, van Aesch YM, Schelen AM, Antonissen C, et al. Tyrosine-dependent and -independent mechanisms of STAT3 activation by the human granulocyte colony-stimulating factor (G-CSF) receptor are differentially utilized depending on G-CSF concentration. Blood 1999;93:113–24.

Weber-Nordt RM, Riley JK, Greenlund AC, Moore KW, Darnell JE, Schreiber RD. Stat3 recruitment by two distinct ligand-induced, tyrosine-phosphorylated docking sites in the interleukin-10 receptor intracellular domain. J Biol Chem 1996;271:27954–61.

Wolk K, Haugen HS, Xu W, Witte E, Waggie K, Anderson M, et al. IL-22 and IL-20 are key mediators of the epidermal alterations in psoriasis while IL-17 and IFN-gamma are not. J Mol Med (Berl) 2009;87:523–36.

Wolk K, Kunz S, Witte E, Friedrich M, Asadullah K, Sabat R. IL-22 increases the innate immunity of tissues. Immunity 2004;21:241–54.

Wolk K, Witte E, Wallace E, Döcke WD, Kunz S, Asadullah K, et al. IL-22 regulates the expression of genes responsible for antimicrobial defense, cellular differentiation, and mobility in keratinocytes: a potential role in psoriasis. Eur J Immunol 2006;36:1309–23.

Xie MH, Aggarwal S, Ho WH, Foster J, Zhang Z, Stinson J, et al. Interleukin (IL)-22, a novel human cytokine that signals through the interferon receptor-related proteins CRF2-4 and IL-22R. J Biol Chem 2000;275:31335–9.

Zheng Y, Danilenko DM, Valdez P, Kasman I, Eastham-Anderson J, Wu J, et al. Interleukin-22, a T(H)17 cytokine, mediates IL-23-induced dermal inflammation and acanthosis. Nature 2007;445:648–51.

Zheng Y, Valdez PA, Danilenko DM, Hu Y, Sa SM, Gong Q, et al. Interleukin-22 mediates early host defense against attaching and effacing bacterial pathogens. Nat Med 2008;14:282–9.

a

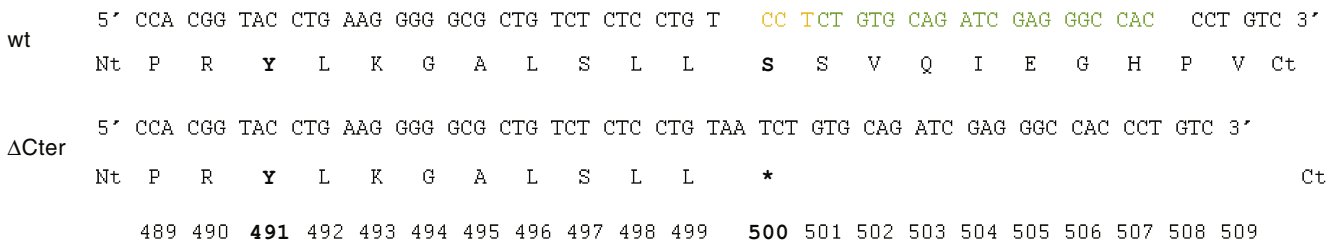

b

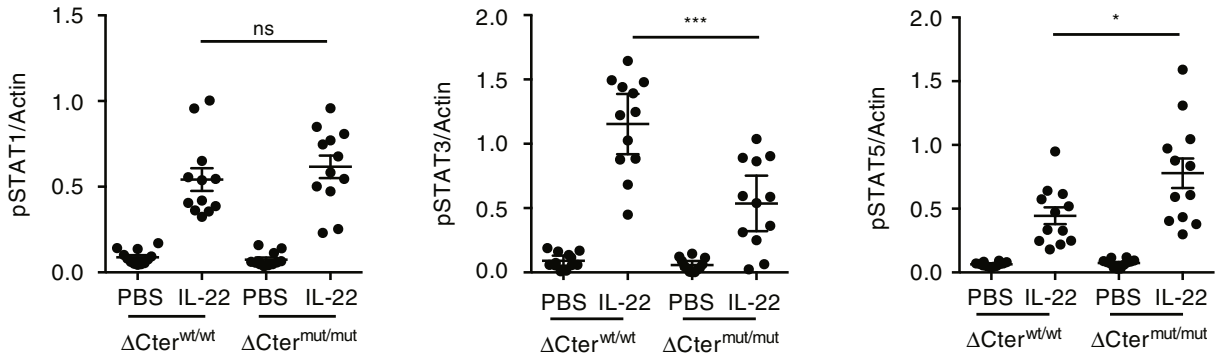

Supplementary Figure S1. The sequence of IL-22R ΔCter and quantification of western blot of Figure 1a. (**a**) The sequence of mouse IL-22Rα (above: WT; below: ΔCter) within (green) the sequence targeted by the guide RNA and (in orange) the PAM sequence. The last Y (Tyr^{491}) and the serine mutated in stop are in bold. (**b**) Quantification of western blot of Figure 1a performed on epidermal cells stimulated for 15 minutes with IL-22 (500 ng/ml). Data are shown as mean ± SEM of four representative experiments. Statistical analyses: Mann Whitney (*$P < 0.05$ and ***$P < 0.001$). IL-22Rα, IL-22 receptor alpha; PAM, protospacer adjacent motif; pSTAT, phosphorylated signal transducer and activator of transcription; WT, wild type.

Supplementary Figure S2. The C-ter part of IL-22Rα does not play a major role in IL-22 activities in the colon. (**a–c**) ΔCter$^{mut/mut}$ mice and control littermate mice were treated intraperitoneally with PBS or IL-22 for 1 hour. (**a**) Western blot analysis of IL-22 signaling in the colon. Total protein lysates from the colon were analyzed by western blot using antibodies directed against total or phosphorylated STAT3. The membranes were then reprobed with an anti–β-actin antibody. Blots are representative of two independent experiments (n = 3 mice per group in each experiment). (**b**) Colon was analyzed by RT-qPCR. One hour after PBS or IL-22 injection, the colon was dissected, and RNA was extracted. *Reg3b* gene expression is normalized against that of β-actin. Data are presented as induction compared with PBS injection. Data are shown as mean ± SEM (n = 5 mice per group). These data are representative of two independent experiments. Statistical analyses: Kruskal–Wallis $*P < 0.05$. C-ter, C-terminal; IL-22Rα, IL-22 receptor alpha; ns, not significant; pSTAT, phosphorylated signal transducer and activator of transcription; STAT, signal transducer and activator of transcription.

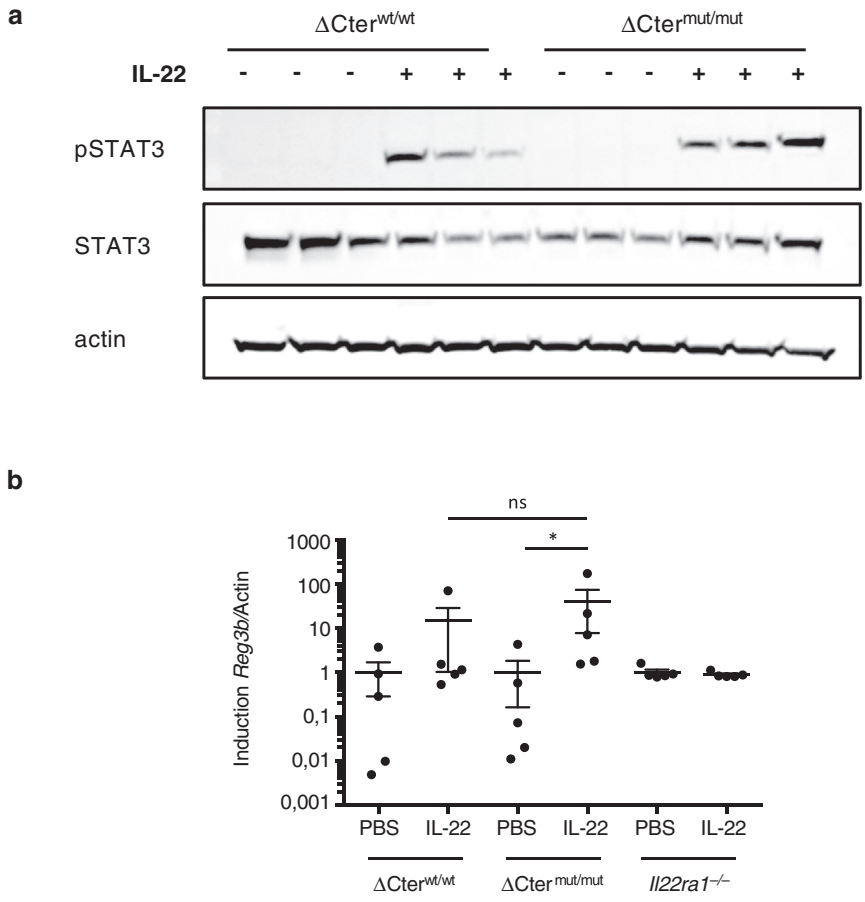

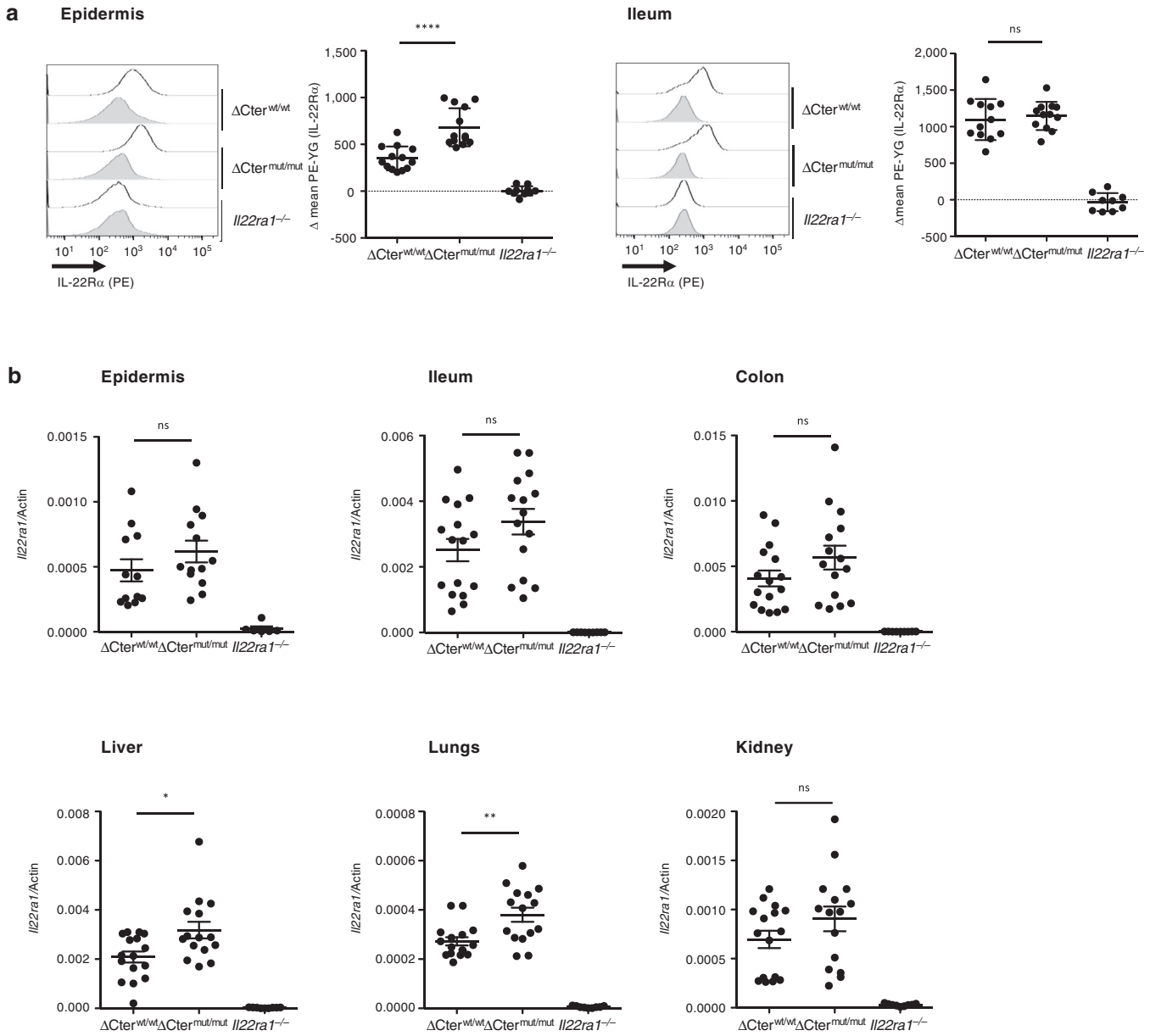

Supplementary Figure S3. IL-22Rα expression analysis by flow cytometry and RT-qPCR. (**a**) Flow cytometry analysis of IL-22Rα in epidermal and intestinal epithelial cells. Cells were gated on living $CD45^{-}$ cells, and IL-22Rα staining was analyzed in $CK10^{+}$ or $EpCAM^{+}$ cells. *Il22ra1*$^{-/-}$ mice were used as a negative control. The grey curve indicates Goat anti-mouse Ab only, and the empty curve indicates IL-22Rα staining. Staining was quantified using delta mean between stained and not stained cells. Data are shown as mean ± SEM and are pooled from three independent experiments (n = 4–5 mice per group in each experiment). (**b**) *Il22ra1* expression was analyzed by RT-qPCR in the epidermal cells, ileum, colon, liver, lung, and kidney. *Il22ra1* gene expression is normalized against that of β-actin. Data are shown as mean ± SEM and are pooled from three independent experiments (n = at least 5 mice per group in each experiment). Statistical analyses: Mann–Whitney (*$P < 0.05$, **$P < 0.01$, and ****$P < 0.0001$). Ab, antibody; EpCAM, epithelial cell adhesion molecule; IL-22Rα, IL-22 receptor alpha; ns, not significant.

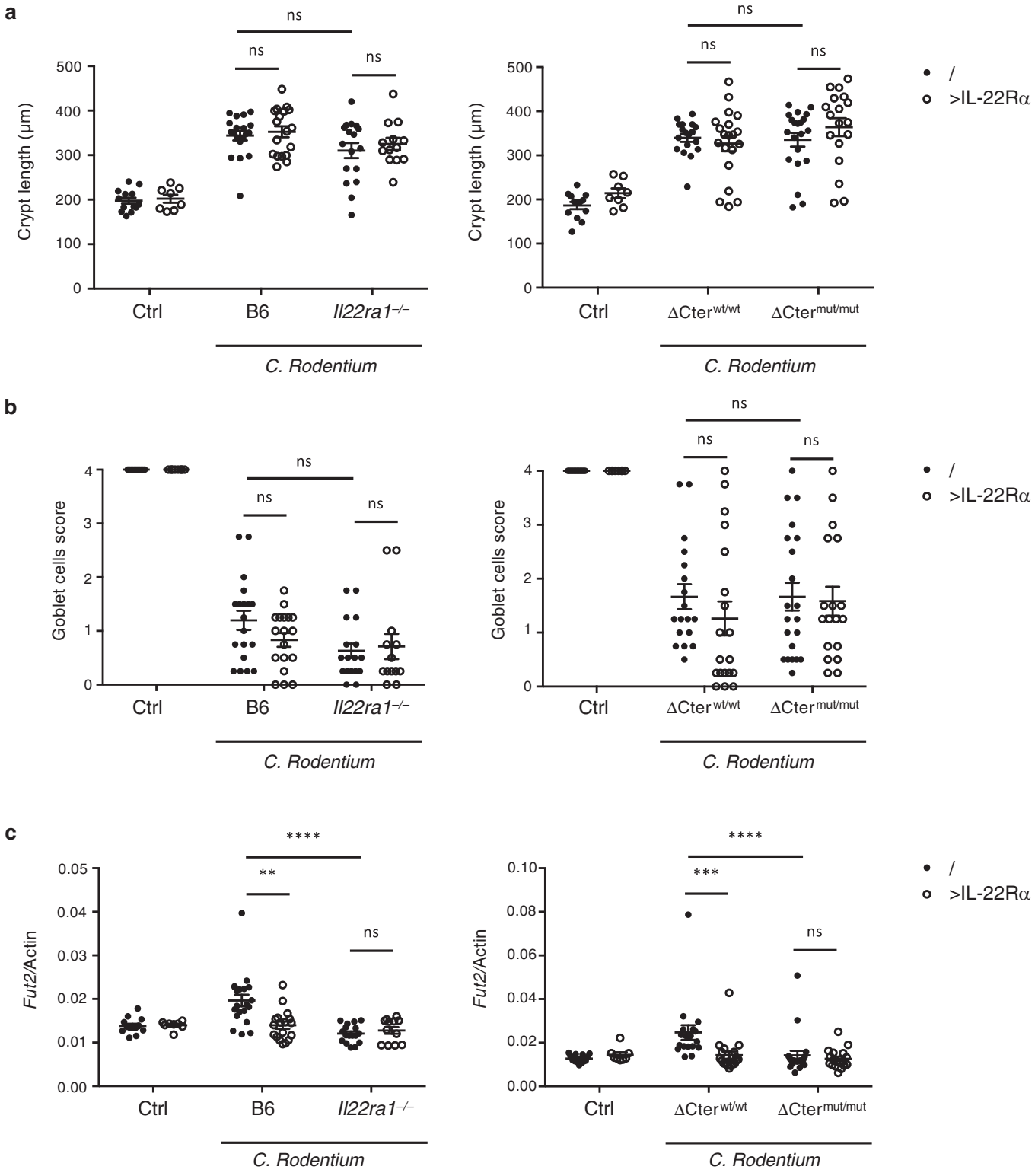

Supplementary Figure S4. Evaluation of colitis on H&E sections and by RT-qPCR. (**a–c**) Mice were orally infected with 2 x 10^9 CFU of *C. rodentium* and intraperitoneally injected with anti–IL-22Rα antibodies (100 µg/mice) 1 day before gavage and each 3 to 4 d (d2, d5, d9). (**a, b**) Evaluation of colitis on H&E sections of the colon by (**a**) measuring crypt length and (**b**) scoring the number of goblet cells. (**c**) *Fut2* expression analysis in the colon, normalized against that of β-actin gene. (**a**–**c**) Data are shown as mean ± SEM and are pooled from three independent experiments (n = min 6 mice per group in each experiment). Statistical analyses: Kruskal–Wallis (**$P < 0.01$, ***$P < 0.001$, and ****$P < 0.0001$). CFU, colony-forming unit; Ctrl, control; IL-22Rα, IL-22 receptor alpha; ns, not significant.

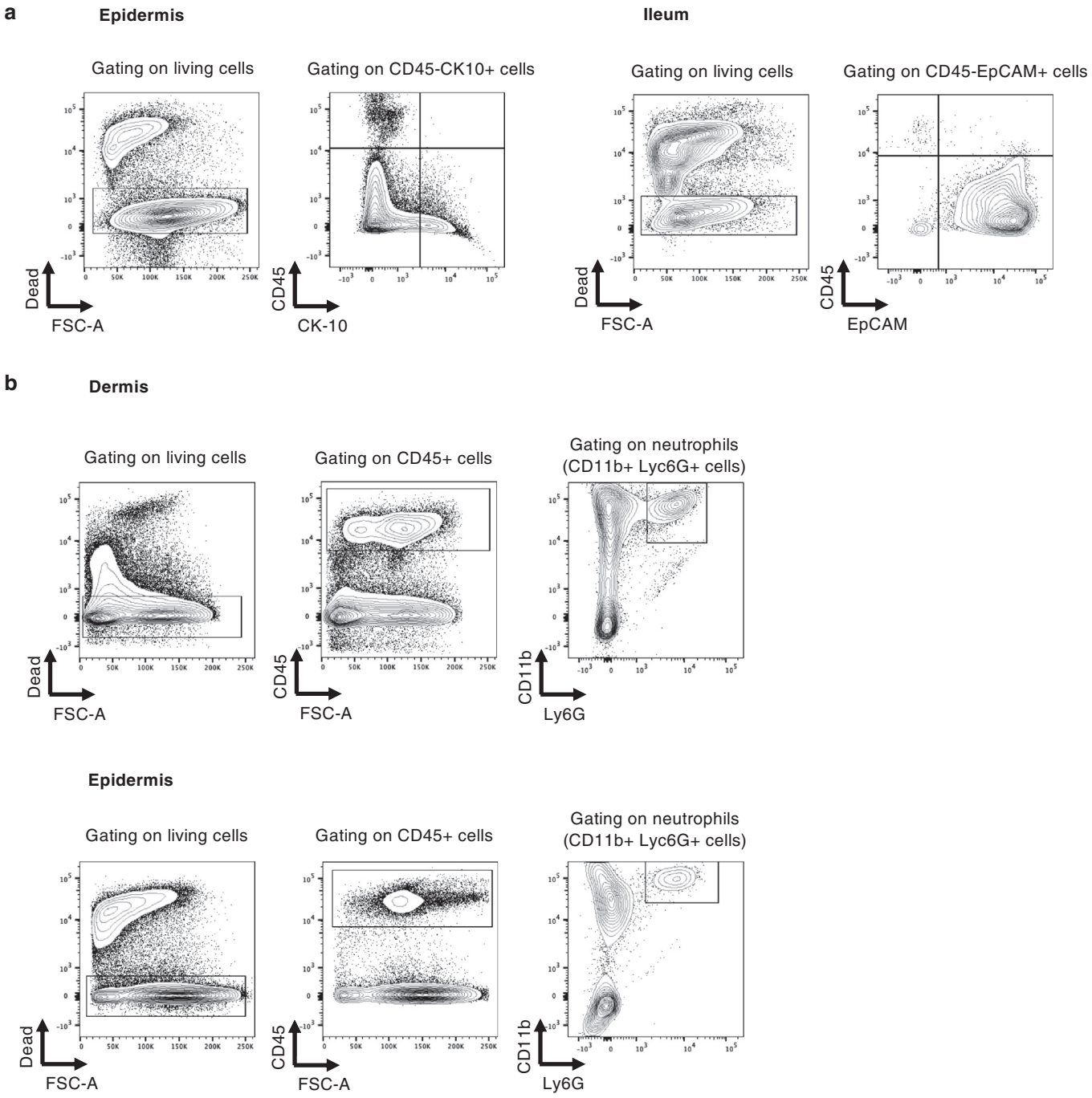

Supplementary Figure S5. Flow cytometry gating strategies. (**a**) Gating strategy for Supplementary Figure S3. Epidermal and epithelial intestinal cells were first gated on living cells and then on $CD45^{-}CK10^{+}$ cells and $CD45^{-}EpCAM^{+}$ cells, respectively. (**b**) Gating strategy of Figure 4g and h. Mice were treated daily with imiquimod on the ears for 7 consecutive days. Epidermal or dermal cells were gated on living cells and then on $CD45^{+}$, and neutrophils were selected for their expression of CD11b and Ly6G. epCAM, epithelial cell adhesion molecule; FSC-A, forward scatter area.

Supplementary Table S1. The sequence of gRNA and ssDNA Designed for CRISPR/Cas9

Primer	Sequence (5′–3′)
gRNA	GTGGCCCTCGATCTGCACAG
ssDNA	ACAGACAGAGGACCTGACCTTCACACACTGCGCAGTGAGGAACCAGAGACA CCACGGTACCTGAAGGGGGCGCTGTCTCTCCTGTAATCTGTGCAGATCGAGGGCCACCCTGTCTCCCTCCCTTTG

Abbreviations: gRNA, guiding RNA; ssDNA, single-strand DNA.

Supplementary Table S2. Antibodies for FACS and Western Blot

Antibodies	Conjugated	Clone or Ref	Manufacturer
Anti-CD45	PerCP or Pe/Cy7	30-F11	BioLegend
Anti-Ly6G/C	FITC	Gr1	BioLegend
Anti-CD4	PE-Cy7	GK1.5	BioLegend
Anti-CD8α	BV421	53-6.7	BioLegend
Anti-TCRb	APC	H57-597	BioLegend
Anti-CD326/EpCAM	PerCP	G8.8	BioLegend
Anti-gd	BV510	GL3	BioLegend
Anti-CD11b	PE	M1/70	BD Biosciences
Anti-cytokeratin-10	PerCP	SPM 261	Novus Bio
Anti-pY701 STAT1		#9167	Cell signaling
Anti-STAT1		#9172	Cell signaling
Anti-pY705 STAT3		#9131	Cell signaling
Anti-STAT3		#12640	Cell signaling
Anti-pY694 STAT5		#9351	Cell signaling
Anti-STAT5		#9363	Cell signaling
Anti-pY1034/1035 Jak1		#331	Cell signaling
Anti-Jak1		#3332	Cell signaling
Anti-pERK		#9101	Cell signaling
Anti–β-actin		A5441	Sigma

Abbreviations: APC, allophycocyanin; epCAM, epithelial cell adhesion molecule; pERK, phosphorylated extracellular signal–regulated kinase; Ref, reference; STAT, signal transducer and activator of transcription.

Supplementary Table S3. RT-qPCR Primer and Probe Sequences

Gene	Primer Forward (5′–3′)	Primer Reverse (5′–3′)	Probe (5′–3′)
Actin	CTCTGGCTCCTAGCACCATGAAG	GCTGGAAGGTGGACAGTGAG	ATCGGTGGCTCCATCCTGGC
Cxcl3	CCATCCAGAGCTTGACGGTGAC	TGGACTTGCCGCTCTTCAGTATC	—
Fut2	AGTCTTCGTGGTTACAAGCAAC	TGGCTGGTGAGCCCTCAATA	—
Gob5	ACTAAGGTGGCCTACCTCCAA	GGAGGTGACAGTCAAGGTGAG	—
Il22ra1	CACACCGGTCCTCTCGGAAG	GGCACTTTCCTTGGACAATATCGG	CACCTACCAGATGCACCTTGAAG
Reg3b	CTACTGCCTTAGACCGTGCTTTC	GAGTCTTCACATTTTGTCCCTTGTC	GTGAAGTTGCCCTATGTCTGC
Reg3g	GAGTGGAGCAATGCTGATGTGATG	GGGATCTTGCTTGTGGCTAGG	—
S100a8	CACCATGCCCTCTACAAGAATGA	CTCTGCTACTCCTTGTGGCTGT	CCTTGCGATGGTGATAAAAGTGGGTGTGGC
Saa1-2	TCTGCTCCCTGCTCCTGGGA	TGGCTTCCTGGTCAGCCATG	—
Socs3	GCCTCGGGGACCATAGGA	GCATCCCGGGGAGCTAGT	—